

Article

***In Situ* Synthesis of Bimetallic Hybrid Nanocatalysts on a Paper-Structured Matrix for Catalytic Applications**

Hiroataka Koga ^{1,*}, Yuuka Umemura ² and Takuya Kitaoka ^{2,3}

¹ Department of Biomaterials Sciences, Graduate School of Agricultural and Life Sciences, The University of Tokyo, 1-1-1 Yayoi, Bunkyo-ku, Tokyo 113-8657, Japan

² Department of Agro-Environmental Sciences, Graduate School of Bioresource and Bioenvironmental Sciences, Kyushu University, 6-10-1 Hakozaki, Higashi-ku, Fukuoka 812-8581, Japan; E-Mails: azurer@agr.kyushu-u.ac.jp (Y.U.); tkitaoka@agr.kyushu-u.ac.jp (T.K.)

³ Biotron Application Center, Kyushu University, 6-10-1 Hakozaki, Higashi-ku, Fukuoka 812-8581, Japan

* Author to whom correspondence should be addressed; E-Mail: ahkoga@mail.ecc.u-tokyo.ac.jp; Tel./Fax: +81-3-5841-5271.

Received: 25 September 2011; in revised form: 14 November 2011 / Accepted: 18 November 2011 / Published: 25 November 2011

Abstract: Bimetallic nanoparticles have attracted significant attention as their electrochemical and catalytic properties being superior to those of the individual component nanoparticles. In this study, gold-silver hybrid nanoparticles (AuAgNPs) with an Au_{core}-Ag_{shell} nanostructure were successfully synthesized on zinc oxide (ZnO) whiskers. The as-prepared nanocatalyst, denoted AuAgNPs@ZnO whisker, exhibits an excellent catalytic efficiency in the aqueous reduction of 4-nitrophenol to 4-aminophenol; the turnover frequency was up to 40 times higher than that of each component nanoparticle. Their unique features were attributed to the electronic ligand effect at the bimetallic interface. In addition, the AuAgNPs were synthesized on a ZnO whisker-containing paper with a fiber-network microstructure, which was prepared via a papermaking technique. The paper-structured AuAgNPs composite possessed both a paper-like practical utility and a good catalytic performance. Furthermore, the on-paper synthesis process for these bimetallic nanocatalysts is facile. These easy-to-handle nanocatalyst hybrid composites are expected to find a wide range of applications in various chemical and catalytic processes.

Keywords: gold; silver; bimetallic nanoparticles; zinc oxide whisker; paper-structured catalyst

1. Introduction

Metal catalysts play a key role in a wide range of chemical industries, since they enable the environmentally friendly conversion of various chemical substances. The recent escalation of energy, environmental and resource issues has led to the ever increasing importance of catalytic processes. Thus, extensive efforts have been devoted to the development of high-performance catalytic materials that can promote desired reactions more effectively and selectively [1–3]. In particular, nano-sized metal particles attract increasing attention as highly active heterogeneous catalysts, due to their unique electronic properties and extremely large specific surface areas [4,5]. For example, gold nanoparticles (AuNPs) exhibit good catalytic activities in various chemical reactions [6–12], such as the reduction of 4-nitrophenol (4-NP) to 4-aminophenol (4-AP), which is a useful intermediate for the production of analgesic and antipyretic drugs, in the liquid phase [10], and the low-temperature oxidation of carbon monoxide (CO) in the gas phase [11], even though ordinary bulk Au is known to be an inefficient catalyst [13,14].

In recent years, there has been a growing interest in bimetallic hybrid NPs, since their chemical and physical properties are different from those for both the bulk metals and their monometallic NP counterparts [15–20]. Toshima *et al.* have reported that core-shell bimetallic NPs exhibit a higher catalytic activity than the monometallic counterparts because the catalytic activity of the shell atoms can be electronically influenced by the core atoms [21–25]. A variety of techniques to tailor bimetallic nanostructures have been investigated, including simultaneous or successive chemical reductions of two types of metal ion [22,26]; it has been reported that platinum (Pt)_{core} bimetallic Pt/Au_{shell} NPs were successfully prepared via the multi-step reduction of HAuCl₄ and H₂PtCl₆ [27]. However, the practical implementation of such metal nanomaterials is challenging, since they are hard to handle. Furthermore, they readily aggregate, resulting in a reduction in surface area and the formation of ordinary bulk metals. This consequently deteriorates their excellent functionality. Thus, the challenge is to establish an efficient and practical immobilization technique that enables highly active metal nanomaterials to be supported onto easy-to-handle matrices.

In our previous reports, the facile and direct *in situ* synthesis of metal NPs, such as copper (Cu) NPs [28–30], silver (Ag) NPs [31,32], PtNPs [29,30,33] and AuNPs [30,34,35], has been achieved using an easy-to-handle paper matrix, composed of ceramic fibers as the main framework and zinc oxide (ZnO) whiskers as a selective scaffold for the synthesis of metal NPs. For example, the “on-paper” synthesis of AuNPs was successfully achieved as follows [30,34,35]: Firstly, ZnO whiskers are incorporated into a ceramic paper matrix using our established papermaking technique. The ZnO whisker-containing paper composite (ZnO paper) is then simply immersed in an aqueous solution of HAuCl₄, leading to the selective formation of AuNPs on the ZnO whiskers. The as-prepared paper composite, denoted as AuNPs@ZnO paper, is like a flexible and easy-to-handle cardboard, and possesses a porous fiber-network microstructure. In both the liquid-phase 4-NP reduction process and the gas-phase CO oxidation process, the AuNPs@ZnO paper exhibited excellent practical utility and high catalytic reactivity [30,34,35]. This facile technique can be extended to various metal NPs, and thus has potential applicability for the on-paper synthesis of bimetallic hybrid nanocatalysts for further functionalization.

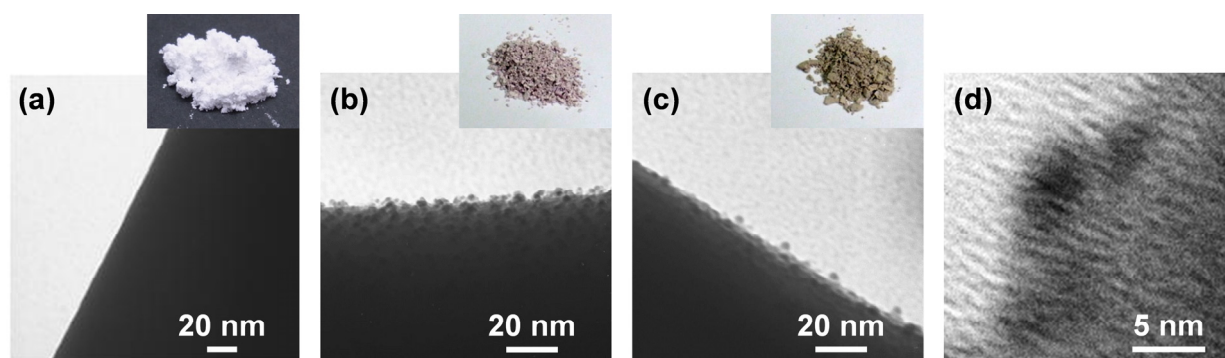
In the present study, the synthesis of Au_{core}-Ag_{shell} bimetallic NPs, denoted as AuAgNPs, on ZnO whiskers was investigated. The on-paper synthesis of AuAgNPs was also conducted. The catalytic performance of the as-prepared AuAgNPs@ZnO whiskers and paper were evaluated in the liquid-phase reduction of 4-NP.

2. Results and Discussion

2.1. AuAgNPs Synthesis on the ZnO Whiskers

ZnO whiskers were added to a neutral solution of HAuCl₄ and the suspension was heated at reflux at 100 °C for 48 h before filtration. The treated whiskers were thoroughly washed with deionized water, dried and calcined at 300 °C for 4 h. The ZnO whiskers then changed color from white to pink-purple, as shown in Figure 1(a,b). Furthermore, transmission electron microscopy (TEM) analysis suggested that many NPs with a particle size less than 5 nm were synthesized on the surfaces of the ZnO whiskers (Figure 1(b)). Subsequently, the HAuCl₄-treated whiskers were added to an aqueous solution of AgNO₃ and the suspension was mixed with aqueous solutions of sodium citrate and hydroquinone for 1 h before filtration. The obtained whiskers were thoroughly washed with deionized water and dried at room temperature for 24 h to afford a yellow-brown product (Figure 1(c)). As shown in Figure 1(d), high-resolution TEM imaging of the resulting NPs indicates that there are electron-dense and electron-lucent layers inside and outside the NPs, respectively. The TEM images suggest that many NPs with core-shell nanostructures were synthesized on the ZnO whiskers.

Figure 1. Optical and TEM images for (a) the original ZnO whiskers, and ZnO whiskers treated with (b) HAuCl₄ and (c) HAuCl₄ and AgNO₃; (d) High-resolution TEM images of NPs on ZnO whiskers treated with HAuCl₄ and AgNO₃.



Energy dispersive X-ray spectroscopy (EDS) analysis of the NPs confirms the coexistence of Au and Ag (Figure 2).

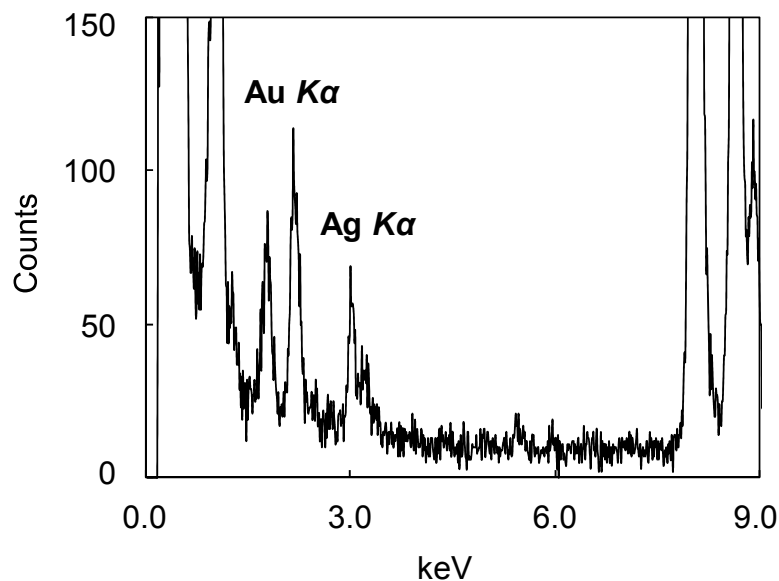
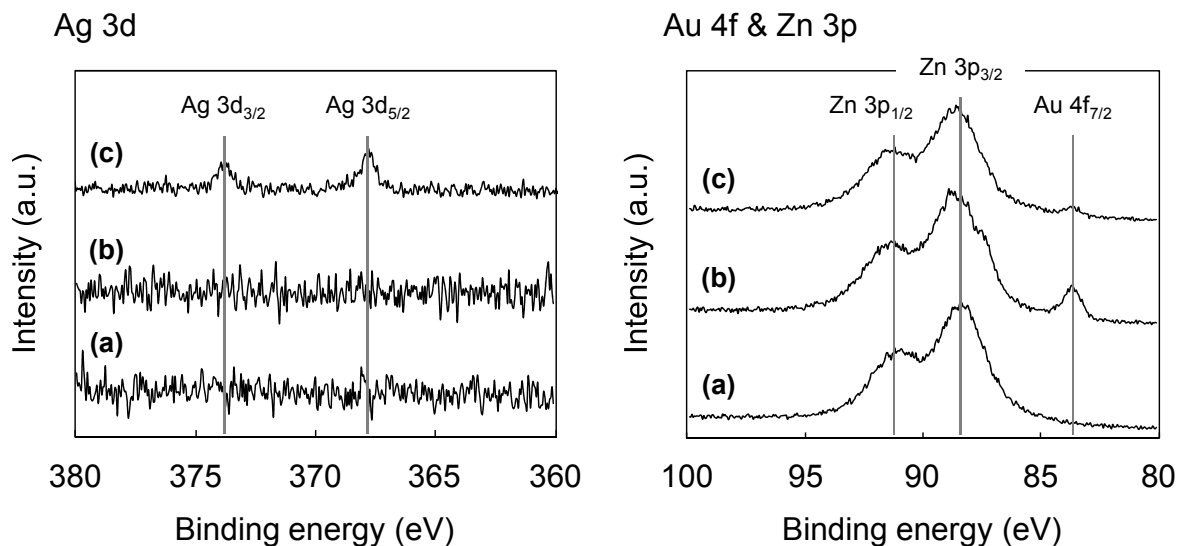
Figure 2. EDS spectrum of NPs on ZnO whiskers treated with H₂AuCl₄ and AgNO₃.

Figure 3 shows the X-ray photoelectron spectroscopy (XPS) spectra for the original ZnO whiskers, ZnO whiskers treated with H₂AuCl₄ and ZnO whiskers treated with H₂AuCl₄ and AgNO₃.

Figure 3. XPS spectra for (a) the original ZnO whiskers, and ZnO whiskers treated with (b) H₂AuCl₄ and (c) H₂AuCl₄ and AgNO₃.

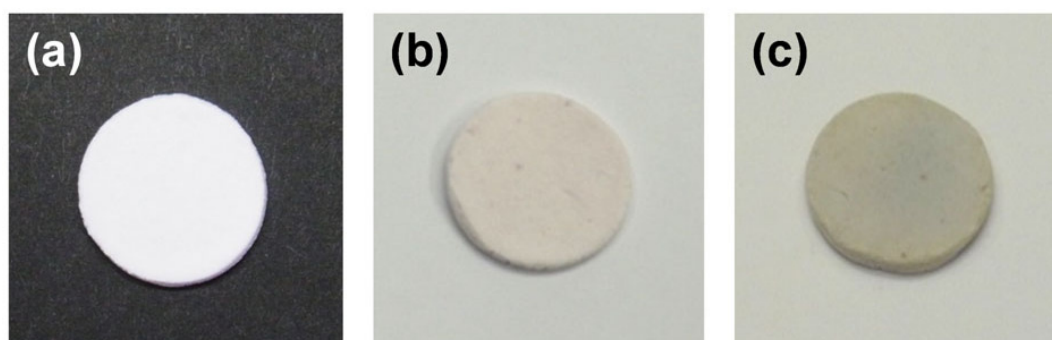
When the ZnO whiskers were treated with H₂AuCl₄, the Au4f_{7/2} peak at *ca.* 83.8 eV, assigned to the characteristic peak of Au(0) [36], appears (Figure 3(b)), which indicates the NPs shown in Figure 1(b) correspond to AuNPs. On the basis of previous reports for the synthesis of Au on metal oxides, via a deposition-precipitation method [37,38], it is proposed that the formation of AuNPs on the ZnO whiskers proceeds as follows: (1) Au(III) complex anions in an aqueous solution of H₂AuCl₄ change from [AuCl₄]⁻ to [Au(OH)₄]⁻ at pH 7.5–8.0; (2) the [Au(OH)₄]⁻ ions are adsorbed onto the surfaces of the positively charged ZnO whiskers under neutral conditions [39] due to electrostatic interactions; (3) thermal treatment at 100 °C leads to the formation of Au(OH)₃ on the surfaces of the ZnO

whiskers; and (4) the $\text{Au}(\text{OH})_3$ is thermally reduced to AuNPs under calcination treatment at 300 °C. When the $\text{AuNPs}^{\text{@}}\text{ZnO}$ whiskers are treated with AgNO_3 , sodium citrate and hydroquinone, the two peaks for $\text{Ag}3d_{3/2}$ and $\text{Ag}3d_{5/2}$ at *ca.* 373.9 eV and *ca.* 367.8 eV, respectively, assigned to the characteristic peaks of $\text{Ag}(0)$ [40], appear, and the intensity for the $\text{Au}(0)$ peak at *ca.* 83.8 eV decreases (Figure 3(c)). This indicates the formation of an Ag layer on the surfaces of the AuNPs. Hydroquinone has a weak redox potential ($E^\circ = -0.7$ V vs. NHE) [41], and is therefore unable to reduce the Ag^+ ions that are isolated in solution (Ag^+/Ag^0 , $E^\circ = -1.8$ V). It can, however, reduce Ag^+ in the presence of Ag^0 clusters or NPs ($E^\circ = +0.799$ V vs. NHE) [42,43]. Furthermore, Lim *et al.* have recently reported the successful formation of an Ag_{shell} layer on Au_{core} NPs using hydroquinone as the reducing agent [44]. On the basis of these results and previous reports, it is proposed that $\text{Au}_{\text{core}}\text{-Ag}_{\text{shell}}$ bimetallic NPs, as shown in Figure 1(d), were successfully synthesized on the surfaces of ZnO whiskers via a multi-step process.

2.2. In Situ Synthesis of AuAgNPs onto ZnO Paper

As described above, very small $\text{Au}_{\text{core}}\text{-Ag}_{\text{shell}}$ bimetallic NPs were successfully immobilized onto the ZnO whiskers. However, these as-prepared $\text{AuAgNPs}^{\text{@}}\text{ZnO}$ whiskers were somewhat difficult to handle, since the ZnO whiskers are fine fibers (Figure 1). The proposed on-paper synthesis technique is a promising strategy to solve this issue [30]. In this study, the on-paper synthesis of AuAgNPs was carried out; ZnO whiskers were initially incorporated into an easy-to-handle paper matrix, upon which the AuAgNPs were synthesized *in situ*. Firstly, the ZnO whiskers were embedded into a paper matrix consisting of ceramic, glass and pulp fibers using our established papermaking technique [45]. The dual polyelectrolyte retention system, which involves the sequential addition of cationic and anionic polyelectrolytes, allowed a quantitative retention of the added materials, which included the fine ZnO whiskers. The paper composite was then thermally treated at 700 °C for 30 min to remove the organic pulp fibers and enhance the physical strength by sintering the glass fibers. Subsequently, the AuAgNPs were synthesized *in situ* on the as-prepared ZnO paper in a multi-step preparation process, similar to that for the $\text{AuAgNPs}^{\text{@}}\text{ZnO}$ whiskers. Figure 4 shows optical images for the original ZnO paper, $\text{AuNPs}^{\text{@}}\text{ZnO}$ paper and $\text{AuAgNPs}^{\text{@}}\text{ZnO}$ paper.

Figure 4. Optical images of (a) the original ZnO paper, (b) $\text{AuNPs}^{\text{@}}\text{ZnO}$ paper and (c) $\text{AuAgNPs}^{\text{@}}\text{ZnO}$ paper. The paper composite size is 1.8×10^2 mm².



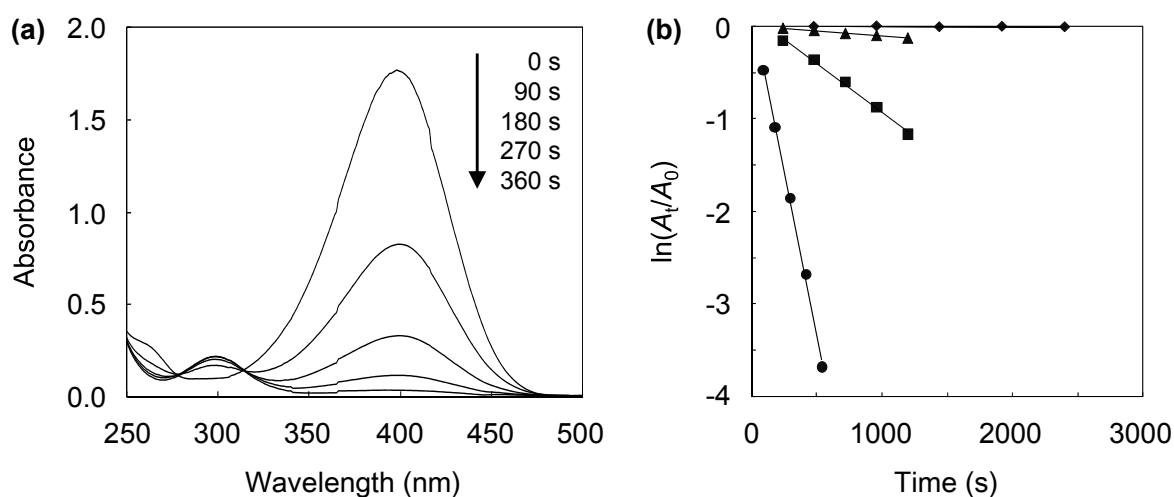
These paper composites are cardboard-like materials. Even after sonication in water for 30 min, no fiber components, including the ZnO whiskers, fell from the paper composites. This suggests that the $\text{AuAgNPs}^{\text{@}}\text{ZnO}$ whiskers are strongly incorporated in the paper matrix and the $\text{AuAgNPs}^{\text{@}}\text{ZnO}$ paper

has a high physical strength. The metal NPs@ZnO paper composites have a highly porous structure; the peak pore size and the porosity are *ca.* 15 μm and *ca.* 80%, respectively [30]. Thus, the AuAgNPs@ZnO paper was porous, flexible and easy-to-handle, allowing excellent practical utility.

2.3. Catalytic Performances of AuAgNPs@ZnO Whisker and Paper

4-NP is known to be an anthropogenic pollutant, since it is carcinogenic, mutagenic, and cyto- and embryonic-toxic. Hence, it is desirable to develop an effective method for the removal of 4-NP. A promising approach involves the catalytic reduction of 4-NP to 4-AP, an important intermediate for the manufacture of analgesic and antipyretic drugs [46]. In this study, the catalytic performances of the AuAgNPs@ZnO whiskers and paper were investigated for the aqueous reduction of 4-NP to 4-AP with NaBH_4 . Figure 5(a) shows the UV-vis absorption spectra recorded throughout the catalytic reduction of 4-NP over the AuAgNPs@ZnO whiskers.

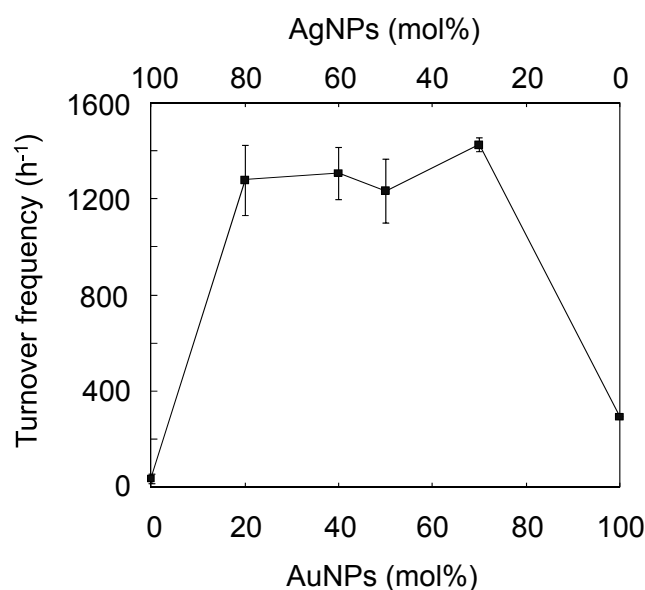
Figure 5. Catalytic performances of the AuAgNPs@ZnO whiskers. (a) UV-vis absorption spectra throughout the catalytic reduction of 4-NP over AuAgNPs@ZnO whiskers, (b) $\ln(A_t/A_0)$ versus reaction time for the reduction of 4-NP; AuAgNPs@ZnO whiskers (circles), AuNPs@ZnO whiskers (squares), AgNPs@ZnO whiskers (triangles) and the original ZnO whiskers (diamonds). A_0 and A_t are the initial absorbance and absorbance at time t at 400 nm. AuAgNPs@ZnO whisker: Au = 0.07 μmol and Ag = 0.03 μmol , AuNPs@ZnO whisker: Au = 0.1 μmol , AgNPs@ZnO whisker: Ag = 0.1 μmol . 4-NP: 15 μmol , NaBH_4 : 3.0 mmol.



The characteristic peak for 4-NP at *ca.* 400 nm, ascribed to the 4-nitrophenolate ion [3,10], gradually decreases, while a new peak at *ca.* 300 nm, assigned to 4-AP [3,10] appears. The reaction with the AuAgNPs@ZnO whiskers was almost complete within 360 s under continuous stirring. Figure 5(b) shows the $\ln(A_t/A_0)$ (A_t : absorbance at 400 nm at the reaction time t , A_0 : absorbance at 400 nm at the initial stage) as a function of reaction time for the AuAgNP@ZnO whiskers, AuNPs@ZnO whiskers, AgNPs@ZnO whiskers and original ZnO whiskers. In each case, a linear correlation was observed, which suggests that the 4-NP reduction, with an excess amount of NaBH_4 , follows pseudo-first-order kinetics [10]. The pseudo-first-order reaction rate constants (k) for the

AuAgNPs@ZnO whiskers, AuNPs@ZnO whiskers, AgNPs@ZnO whiskers and ZnO whiskers were estimated from each slope to be $7.0 \times 10^{-3} \text{ s}^{-1}$, $1.1 \times 10^{-3} \text{ s}^{-1}$, $1.0 \times 10^{-4} \text{ s}^{-1}$ and $3.0 \times 10^{-6} \text{ s}^{-1}$, respectively. The original ZnO whiskers exhibit an extremely low catalytic efficiency, indicating that the metal NPs synthesized onto the ZnO whiskers play a key role in this reaction. The AuNPs@ZnO whiskers demonstrate a higher catalytic efficiency than the AgNPs@ZnO whiskers, suggesting the AuNPs have a superior catalytic activity to the AgNPs. It is noteworthy that the AuAgNPs@ZnO whiskers had the highest catalytic efficiency among the test samples; the k value for the AuAgNPs@ZnO whiskers ($7.0 \times 10^{-3} \text{ s}^{-1}$) was 1.2–3.3 times larger than those for the many metal nanocatalysts previously reported, such as AuNP@cellulose single nanofibers ($5.9 \times 10^{-3} \text{ s}^{-1}$) [3], dendric Ag/Au bimetallic nanostructures ($6.07 \times 10^{-3} \text{ s}^{-1}$) [19], AuNPs/poly(amidoamine) dendrimer ($3.7 \times 10^{-3} \text{ s}^{-1}$) [47] and spongy Au nanocrystals ($2.1 \times 10^{-3} \text{ s}^{-1}$) [48]. Figure 6 shows influence of the Au/Ag ratio on the turnover frequency (TOF) for the AuAgNPs@ZnO whiskers in the reduction of 4-NP.

Figure 6. Turnover frequencies (TOFs) for the AuAgNPs@ZnO whiskers in the reduction of 4-NP, as a function of Au and Ag mol%. The total amount of Au and Ag: 0.1 μmol , 4-NP: 15 μmol , NaBH_4 : 3.0 mmol.

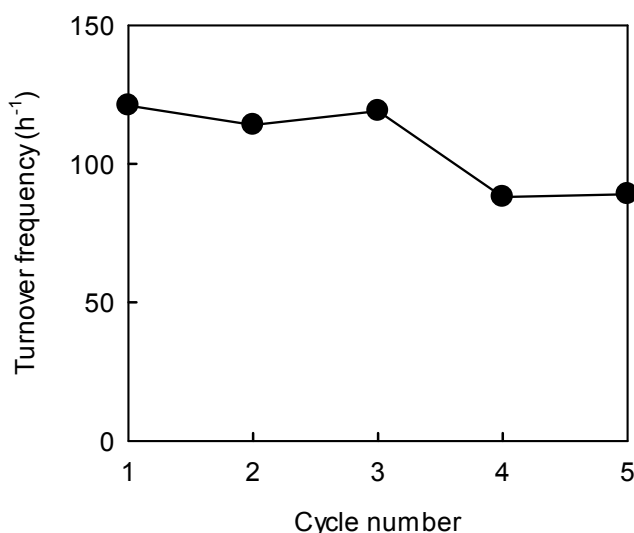


Although the total amount of Au and Ag was constant (0.1 μmol) in all test samples, the Au_{core}-Ag_{shell} bimetallic NPs exhibited a much higher TOF than the monometallic equivalents at all Au/Ag ratios (7/3, 5/5, 4/6, 2/8) studied. The maximum TOF (*ca.* 1400 h⁻¹) was achieved with an Au/Ag ratio of 7/3, and was 5–40 fold higher those for the monometallic NPs. Esumi *et al.* have proposed that the AuNPs-catalyzed 4-NP reduction, with an excess of NaBH_4 , proceeds in two steps: (1) the diffusion and adsorption of 4-NP to catalyst surface; and (2) an electron transfer mediated by the catalyst surface from BH_4^- to 4-NP [47,49]. They concluded that the first step is the rate limiting step in the 4-NP reduction. Thus, the interesting phenomenon observed in this study may be attributed to the electronic ligand effect between the core and shell atoms [21,22,24]. Since the ionization potentials for Ag and Au are 7.58 eV and 9.22 eV, respectively, an electronic transfer could occur from Ag_{shell} to Au_{core} [25], resulting in a decrease in electron density on the shell surfaces of the

Au_{core}-Ag_{shell} bimetallic hybrid NPs. Such electron-deficient surfaces would favor the adsorption of 4-nitrophenolate anions, and lead to excellent 4-NP reduction efficiencies.

Figure 7 shows the 4-NP reduction performance for the AuAgNPs@ZnO paper.

Figure 7. Reusability of AuAgNPs@ZnO paper in the 4-NP reduction. Total amount of Au and Ag: 0.01 μmol (Au = 0.007 μmol and Ag = 0.003 μmol), 4-NP: 15 μmol , NaBH₄: 3.0 mmol.



The reusability of the AuAgNPs@ZnO paper was evaluated from the changes in TOF over a five-cycle test: the sequential procedure for the 4-NP reduction reaction involved washing with water and drying at room temperature between each cycle of the test. The TOF value for the AuAgNPs@ZnO paper was *ca.* 120 h^{-1} in the first cycle, which is lower than that for the AuAgNPs@ZnO whiskers. This may be because the accessibility for the reactants to the AuAgNPs@ZnO paper was insufficient under continuous stirring due to its large size (*ca.* 15 mm in diameter) in comparison to the fine AuAgNPs@ZnO whiskers (fiber length: 2–50 μm , fiber diameter: 0.2–3.0 μm), although the unique porous microstructure of the metal NPs@ZnO paper, with an open porous network throughout, was favorable for the efficient transport of the 4-NP to the NPs surfaces under static conditions [30,35]. While the AuAgNPs@ZnO whiskers exhibited a higher catalytic performance, they remain difficult to handle and hard to separate from the reaction system owing to their fine size (Figure 1(c)). Conversely, the AuAgNPs@ZnO paper is easy-to-handle in practical terms due to its simple paper form (Figure 4(c)), allowing a high reusability. In fact, the AuAgNPs@ZnO paper was easily recovered from the reaction solution after each performance test, and demonstrated a TOF of *ca.* 90 h^{-1} after the fifth cycle. The atomic absorption analysis confirmed that no AuAgNPs dropped out of the paper composite during the catalytic reaction. Thus this decrease in the catalytic efficiency may be due to the inevitable aggregation of metal NPs during the 4-NP reduction [10,35] and/or the degradation of an Au_{core}-Ag_{shell} nanostructure. It is difficult to fully suppress the deterioration of the metal NPs after repeated use, but the immobilization of the AuAgNPs on a paper matrix via our on-paper synthesis technique has provided a high degree of practical utility for the very small AuAgNPs. Furthermore, the highly porous structure of the paper composites provide a great potential for application to flow-type processes, which can be applied to continuous processes, regardless of liquid- [50] and gas-phase reactions [28–30,33,34,45].

Thus the AuAgNPs@ZnO paper with paper-like characteristics is a promising practical material for a variety of catalytic processes.

3. Experimental Section

3.1. Materials

Ceramic fibers (SiO₂: 52 wt%, Al₂O₃: 48 wt%) and ZnO whiskers (fiber length: 2–50 μm, fiber diameter: 0.2–3.0 μm) were obtained from IBIDEN, Ltd. (Tokyo, Japan) and Matsushita Amtec, Ltd. (Osaka, Japan) respectively. Pulp fibers, as a matrix component in the paper fabrication process were prepared by refining a commercial bleached hardwood kraft pulp to a Canadian Standard Freeness of 300 mL with a Technical Association of the Pulp and Paper Industry standard beater. Glass fibers (CMLF208, Nippon Sheet Glass, Ltd., Tokyo, Japan) were used as a binding component to enhance the physical strength of the paper composite following calcination. Two types of flocculants, namely cationic poly(diallyldimethylammonium chloride) (PDADMAC; molecular weight *ca.* 3 × 10⁵ g mol⁻¹; charge density 5.5 meq g⁻¹) and anionic polyacrylamide (A-PAM, HH-351; molecular weight *ca.* 4 × 10⁶ g mol⁻¹; charge density 0.64 meq g⁻¹), were purchased from Aldrich, Ltd. (Sheffield, UK) and Kurita, Ltd. (Tokyo, Japan), respectively. AgNO₃ (99.8+ % purity) and trisodium citrate dihydrate were obtained from Wako Pure Chemical Industries, Ltd. HAuCl₄·3H₂O (99.9% purity), hydroquinone (>99% purity), 4-NP (99% purity) and sodium borohydride (NaBH₄, >95% purity) were purchased from Aldrich, Ltd. (Sheffield, UK). All other chemicals were of reagent grade and used without further purification.

3.2. Preparation of AuAgNPs@ZnO Whiskers

Au_{core}-Ag_{shell} bimetallic NPs were synthesized on ZnO whiskers via a multi-step process. Firstly, the synthesis of the AuNPs onto the ZnO whiskers was conducted using a deposition-precipitation method in line, to some degree to previous reports [37,38]. An aqueous solution of HAuCl₄ (0.2–0.5 mM, 25 mL) was adjusted to pH 7.5–8.0 with aqueous NaOH (100 mM). The ZnO whiskers (1.0 g) were then suspended in the solution, and the mixture was refluxed at 100 °C for 48 h with continuous stirring. The suspension was then filtered, washed with deionized water, dried at 80 °C for 1 h and calcined at 300 °C for 4 h. An Ag nanolayer was formed on the as-synthesized AuNPs as follows. The as-prepared AuNPs@ZnO whiskers (400 mg) were suspended in an aqueous solution of AgNO₃ (0.06–0.55 mM, 5 mL) for 30 min. Aqueous solutions of sodium citrate (1.0% (w/v), 50 μL), as a stabilizer, and hydroquinone (30 mM, 200 μL), as a reducing agent, were then added to the mixture, followed by stirring for 1 h and filtration. Finally, the products were thoroughly washed with deionized water and dried at room temperature for 24 h. The AgNPs@ZnO whiskers were also prepared according to our previous report [31].

3.3. Preparation of ZnO Paper by a Papermaking Technique

The preparation of paper composites using organic and inorganic fibers, via a dual polyelectrolyte retention system, was conducted according to our previous reports [30,45]. In summary, an aqueous suspension of ceramic fibers, glass fibers and ZnO whiskers was mixed with PDADMAC (0.5 wt% of

total solids) and A-PAM (0.5 wt% of total solids), in that order. This mixture was then added to a water suspension of pulp fibers, and solidified through dewatering using a 200-mesh wire. The wet-state handsheets were pressed at 350 kPa for 3 min and dried at 105 °C for 1 h. The resulting paper composite, with an area of 2×10^4 mm² and a thickness of 1.4 mm, was composed of ceramic fibers (4.0 g), glass fibers (4.0 g), ZnO whiskers (1.0 g) and pulp fibers (1.0 g). The obtained paper composites were thermally treated at 700 °C for 30 min to remove any pulp fibers and to improve the physical strength through the sintering of glass fibers.

3.4. Preparation of AuAgNPs@ZnO Paper

The *in situ* synthesis of AuAgNPs onto the ZnO paper was performed in a similar manner to that for the AuAgNPs@ZnO whiskers. An aqueous solution of HAuCl₄ (0.03 mM, 80 mL) was adjusted to pH 7.5–8.0 using an aqueous solution of NaOH (100 mM). The ZnO paper was cut into circular pieces, each with an area of 1.8×10^2 mm² and a thickness of 1.4 mm. The four pieces were immersed in the solution and stirred at reflux for 48 h. The treated paper discs were removed from the solution using tweezers, thoroughly washed with deionized water, dried at 80 °C for 1 h and calcined at 300 °C for 4 h. A piece of the as-prepared AuNPs@ZnO paper was then immersed in an aqueous solution of AgNO₃ (0.001 mM, 5 mL) for 30 min. Aqueous solutions of sodium citrate (1.0% (w/v), 50 µL) and hydroquinone (30 mM, 200 µL) were added to the mixture and stirred for 1 h. The obtained paper disc was thoroughly washed with deionized water and dried at room temperature for 24 h.

3.5. Catalytic Performance Test

Catalytic performances towards the reduction of 4-NP were investigated in batch mode. An aqueous solution of 4-NP (0.1 mM, 150 mL) was initially mixed with NaBH₄ (3.0 mmol), as the reducing agent. The AuNPs@ZnO whiskers, AgNPs@ZnO whiskers or AuAgNPs@ZnO whiskers were then added to the solution. In all cases, the total amount of Au and Ag remained constant at 0.1 µmol. Reactions were carried out at 25 °C with continuous stirring. At given times, samples (1.0 mL) were taken, filtered through a 0.2 µm membrane filter (Chromatodisk, GL Sciences, Ltd.) and analyzed via UV-vis. UV-vis spectra of the reaction solutions (1.0 mL) were recorded at room temperature using a U-3000 spectrophotometer (Hitachi, Japan). According to a previous report [10], the rate constants for the reduction process were determined by measuring the change in absorbance at 400 nm as a function of time. The reusability of the AuAgNPs@ZnO paper was also evaluated from the changes in TOF value during a five-cycle test: the sequential procedures of the 4-NP reduction reaction, washing with water and drying at room temperature were conducted in each cycle of the test.

3.6. Analyses

The levels of Au and Ag were determined using atomic absorption spectrophotometry on a Shimadzu AA-6600F instrument. TEM and EDS analyses were performed using a JEM-2010FEF instrument (JEOL, Ltd., Tokyo, Japan) at a 200 kV accelerating voltage. The chemical states of the component elements were analyzed by XPS (AXIS-HSi spectrometer, Shimadzu/Kratos, Ltd., Kyoto, Japan) using a monochromatic AlK α X-ray source (1486.6 eV) with a 12 kV voltage and 10 mA current. The

binding energies for all spectra were determined with respect to the C1s reference signal (unoxidized C-C bond) at 285.0 eV.

4. Conclusions

We have demonstrated the successful synthesis of Au-Ag bimetallic hybrid NPs with Au_{core}-Ag_{shell} nanostructures on ZnO whiskers. The AuAgNPs@ZnO whiskers exhibit an excellent catalytic efficiency in the aqueous reduction of 4-NP to 4-AP: the TOF for the AuAgNPs@ZnO whiskers was 5–40 fold higher than those for the monometallic equivalents. This may be caused by the electronic ligand effect. Electron-deficient shell surfaces, derived from Au_{core}-Ag_{shell} nanostructures, would be advantageous in the adsorption of 4-nitrophenolate anions, which would lead to an excellent 4-NP reduction efficiency. The on-paper synthesis of the AuAgNPs was also accomplished, and the resulting AuAgNPs@ZnO paper had paper-like characteristics and possessed an excellent practical utility. Thus, the on-paper synthesis of bimetallic NPs is a promising technique to potentially promote the practical use of highly-functional bimetallic nanocatalysts across a wide range of chemical industries.

Acknowledgments

This research was supported by a Research Fellowship for Young Scientists from the Japan Society for the Promotion of Science (H.K.).

References

1. Cortright, R.D.; Davda, R.R.; Dumesic, J.A. Hydrogen from catalytic reforming of biomass-derived hydrocarbons in liquid water. *Nature* **2002**, *418*, 964–967.
2. Nishihata, Y.; Mizuki, J.; Akao, T.; Tanaka, H.; Uenishi, M.; Kimura, M.; Okamoto, T.; Hamada, N. Self-regeneration of a Pd-perovskite catalyst for automotive emissions control. *Nature* **2002**, *418*, 164–167.
3. Koga, H.; Tokunaga, E.; Hidaka, M.; Umemura, Y.; Saito, T.; Isogai, A.; Kitaoka, T. Topochemical synthesis and catalysis of metal nanoparticles exposed on crystalline cellulose nanofibers. *Chem. Commun.* **2010**, *46*, 8567–8569.
4. Zhou, B.; Han, S.; Raja, R.; Somorjai, G.A. *Nanotechnology in Catalysis*; Springer Science and Business Media: New York, NY, USA, 2007; Volume 3.
5. Campelo, J.M.; Luna, D.; Luque, R.; Marinas, J.M.; Romero, A.A. Sustainable preparation of supported metal nanoparticles and their applications in catalysis. *ChemSusChem* **2009**, *2*, 18–45.
6. Haruta, M. When gold is not noble: Catalysis by nanoparticles. *Chem. Rec.* **2003**, *3*, 75–87.
7. Bond, G.C.; Louis, C.; Thompson, D.T.; Hutchings, G.J. *Catalysis by Gold*; Imperial College: London, UK, 2006.
8. Hashmi, A.S.K.; Hutchings, G.J. Gold catalysis. *Angew. Chem. Int. Ed.* **2006**, *45*, 7896–7936.
9. Ishida, T.; Haruta, M. Gold catalysts: Towards sustainable chemistry. *Angew. Chem. Int. Ed.* **2007**, *46*, 7154–7156.
10. Kuroda, K.; Ishida, T.; Haruta, M. Reduction of 4-nitrophenol to 4-aminophenol over Au nanoparticles deposited on PMMA. *J. Mol. Catal. A Chem.* **2009**, *298*, 7–11.

11. Wong, K.; Zeng, Q.; Yu, A. Gold catalysts: A new insight into the molecular adsorption and CO oxidation. *Chem. Eng. J.* **2009**, *155*, 824–828.
12. Zhu, Y.; Jin, R.; Sun, Y. Atomically monodisperse gold nanoclusters catalysts with precise core-shell structure. *Catalysts* **2011**, *1*, 3–17.
13. Armer, B.; Schmidbaur, H. Organogoldchemie. *Angew. Chem.* **1970**, *82*, 120–133.
14. Bond, G.C. The catalytic properties of gold. *Gold Bull.* **1972**, *5*, 11–13.
15. Luo, J.; Wang, L.; Mott, D.; Njoki, P.N.; Lin, Y.; He, T.; Xu, Z.; Wanjana, B.N.; Lim, I.; Zhong, C.J. Core/shell nanoparticles as electrocatalysts for fuel cell reactions. *Adv. Mater.* **2008**, *20*, 4342–4347.
16. Chiang, W.H.; Sankaran, R.M. Synergistic effects in bimetallic nanoparticles for low temperature carbon nanotube growth. *Adv. Mater.* **2008**, *20*, 4857–4861.
17. Xu, C.X.; Wang, L.Q.; Wang, R.Y.; Wang, K.; Zhang, Y.; Tian, F.; Ding, Y. Nanotubular mesoporous bimetallic nanostructures with enhanced electrocatalytic performance. *Adv. Mater.* **2009**, *21*, 2165–2169.
18. Zhang, Q.B.; Xie, J.P.; Liang, J.; Lee, J.Y. Synthesis of monodisperse Ag-Au alloy nanoparticles with independently tunable morphology, composition, size, and surface chemistry and their 3-D superlattices. *Adv. Funct. Mater.* **2009**, *19*, 1387–1398.
19. Huang, J.; Vongehr, S.; Tang, S.; Lu, H.; Shen, J.; Meng, X. Ag dendrite-based Au/Ag bimetallic nanostructures with strongly enhanced catalytic activity. *Langmuir* **2009**, *25*, 11890–11896.
20. Peng, X.; Pan, Q.; Rempel, G.L.; Wu, S. Synthesis, characterization, and application of PdPt and PdRh bimetallic nanoparticles encapsulated within amine-terminated poly(amidoamine) dendrimers. *Catal. Commun.* **2009**, *11*, 62–66.
21. Toshima, N.; Harada, M.; Yonezawa, T.; Kushihashi, K.; Asakura, K. Structural-analysis of polymer-protected Pd/Pt bimetallic clusters as dispersed catalysts by using extended X-ray absorption fine-structure spectroscopy. *J. Phys. Chem.* **1991**, *95*, 7448–7453.
22. Toshima, N.; Yonezawa, T. Bimetallic nanoparticles—Novel materials for chemical and physical applications. *New J. Chem.* **1998**, *22*, 1179–1201.
23. Matsushita, T.; Shiraishi, Y.; Horiuchi, S.; Toshima, N. Synthesis and catalysis of polymer-protected Pd/Ag/Rh trimetallic nanoparticles with a core-shell structure. *Bull. Chem. Soc. Jpn.* **2007**, *80*, 1217–1225.
24. Toshima, N.; Ito, R.; Matsushita, T.; Shiraishi, Y. Trimetallic nanoparticles having a Au-core structure. *Catal. Today* **2007**, *122*, 239–244.
25. Tokonami, S.; Morita, N.; Takasaki, K.; Toshima, N. Novel synthesis, structure, and oxidation catalysis of Ag/Au bimetallic nanoparticles. *J. Phys. Chem. C* **2010**, *114*, 10336–10341.
26. Kim, M.J.; Lee, K.Y.; Jeong, G.H.; Jang, J.; Han, S.W. Fabrication of Au-Ag alloy nanoprisms with enhanced catalytic activity. *Chem. Lett.* **2007**, *36*, 1350–1351.
27. Dai, J.; Yao, P.; Hua, N.; Yang, P.; Du, Y. Preparation and characterization of polymer-protected Pt[@]Pt/Au core-shell nanoparticles. *J. Dispersion Sci. Technol.* **2007**, *28*, 872–875.
28. Koga, H.; Kitaoka, T.; Wariishi, H. *In situ* synthesis of Cu nanocatalysts on ZnO whiskers embedded in a microstructured paper composite for autothermal hydrogen production. *Chem. Commun.* **2008**, 5616–5618.

29. Koga, H.; Umemura, Y.; Kitaoka, T. Design of catalyst layers by using paper-like fiber/metal nanocatalyst composites for efficient NO_x reduction. *Compos. Part B* **2011**, *42*, 1108–1113.
30. Koga, H.; Kitaoka, T. On-paper synthesis of metal nanoparticles for catalytic applications. *Sen'i Gakkaishi* **2011**, *67*, 141–152.
31. Koga, H.; Kitaoka, T.; Wariishi, H. *In situ* synthesis of silver nanoparticles on zinc oxide whiskers incorporated in a paper matrix for antibacterial applications. *J. Mater. Chem.* **2009**, *19*, 2135–2140.
32. Koga, H.; Kitaoka, T. *Silver Nanoparticles*; IN-TECH Education and Publishing KG: Vienna, Austria, 2010.
33. Koga, H.; Umemura, Y.; Tomoda, A.; Suzuki, R.; Kitaoka, T. *In situ* synthesis of platinum nanocatalysts on a microstructured paperlike matrix for the catalytic purification of exhaust gases. *ChemSusChem* **2010**, *3*, 604–608.
34. Koga, H.; Kitaoka, T.; Wariishi, H. On-paper synthesis of Au nanocatalysts from Au(III) complex ions for low-temperature CO oxidation. *J. Mater. Chem.* **2009**, *19*, 5244–5249.
35. Koga, H.; Kitaoka, T. One-step synthesis of gold nanocatalysts on a microstructured paper matrix for the reduction of 4-nitrophenol. *Chem. Eng. J.* **2011**, *168*, 420–425.
36. Qian, K.; Lv, S.; Xiao, X.; Sun, H.; Lu, J.; Luo, M.; Huang, W. Influences of CeO₂ microstructures on the structure and activity of Au/CeO₂/SiO₂ catalysts in CO oxidation. *J. Mol. Catal. A* **2009**, *306*, 40–47.
37. Haruta, M.; Tsubota, S.; Kobayashi, T.; Kageyama, H.; Genet, M.J.; Delmon, B. Low-temperature oxidation of CO over gold supported on TiO₂, α-Fe₂O₃, and Co₃O₄. *J. Catal.* **1993**, *144*, 175–192.
38. Bond, G.C.; Thompson, D.T. Catalysis by gold. *Catal. Rev. Sci. Eng.* **1999**, *41*, 319–388.
39. Muster, T.H.; Cole, I.S. The protective nature of passivation films on zinc: Surface charge. *Corros. Sci.* **2004**, *46*, 2319–2335.
40. Shah, M.S.A.S.; Nag, M.; Kalagara, T.; Singh, S.; Manorama, S.V. Silver on PEG-PU-TiO₂ polymer nanocomposite films: An excellent system for antibacterial applications. *Chem. Mater.* **2008**, *20*, 2455–2460.
41. Gentry, S.T.; Fredericks, S.J.; Krchnavek, R. Controlled particle growth of silver sols through the use of hydroquinone as a selective reducing agent. *Langmuir* **2009**, *25*, 2613–2621.
42. Mostafavi, M.; Marignier, J.L.; Amblard, J.; Belloni, J. Nucleation dynamics of silver aggregates simulation of photographic development processes. *Radiat. Phys. Chem.* **1989**, *34*, 605–617.
43. Linnert, T.; Mulvaney, P.; Henglein, A.; Weller, H. Long-lived nonmetallic silver clusters in aqueous solution: Preparation and photolysis. *J. Am. Chem. Soc.* **1990**, *112*, 4657–4664.
44. Lim, D.-K.; Kim, I.-J.; Nam, J.-M. DNA-embedded Au/Ag core-shell nanoparticles. *Chem. Commun.* **2008**, 5312–5314.
45. Koga, H.; Fukahori, S.; Kitaoka, T.; Tomoda, A.; Suzuki, R.; Wariishi, H. Autothermal reforming of methanol using paper-like Cu/ZnO catalyst composites prepared by a papermaking technique. *Appl. Catal. A* **2006**, *309*, 263–269.
46. Du, Y.; Chen, H.; Chen, R.; Xu, N. Synthesis of p-aminophenol from p-nitrophenol over nano-sized nickel catalysts. *Appl. Catal. A* **2004**, *277*, 259–264.
47. Hayakawa, K.; Yoshimura, T.; Esumi, K. Preparation of gold-dendrimer nanocomposites by laser irradiation and their catalytic reduction of 4-nitrophenol. *Langmuir* **2003**, *19*, 5517–5521.

48. Rashid, M.H.; Bhattacharjee, R.R.; Kotal, A.; Mandal, T.K. Synthesis of spongy gold nanocrystals with pronounced catalytic activities. *Langmuir* **2006**, *22*, 7141–7143.
49. Esumi, K.; Miyamoto, K.; Yoshimura, T. Comparison of PAMAM-Au and PPI-Au nanocomposites and their catalytic activity for reduction of 4-nitrophenol. *J. Colloid Interface Sci.* **2002**, *254*, 402–405.
50. Koga, H.; Kitaoka, T.; Isogai, A. *In situ* modification of cellulose paper with amino groups for catalytic applications. *J. Mater. Chem.* **2011**, *21*, 9356–9361.

© 2011 by the authors; licensee MDPI, Basel, Switzerland. This article is an open access article distributed under the terms and conditions of the Creative Commons Attribution license (<http://creativecommons.org/licenses/by/3.0/>).